Elastic Properties of Isolated Thick Filaments Measured by Nanofabricated Cantilevers

Thomas Neumann, Mark Fauver, and Gerald H. Pollack
Department of Bioengineering, University of Washington, Seattle, Washington 98195 USA

ABSTRACT Using newly developed nanofabricated cantilever force transducers, we have measured the mechanical properties of isolated thick filaments from the anterior byssus retractor muscle of the blue mussel *Mytilus edulis* and the telson levator muscle of the horseshoe crab *Limulus polyphemus*. The single thick filament specimen was suspended between the tip of a flexible cantilever and the tip of a stiff reference beam. Axial stress was placed on the filament, which bent the flexible cantilever. Cantilever tips were microscopically imaged onto a photodiode array to extract tip positions, which could be converted into force by using the cantilever stiffness value. Length changes up to 23% initial length (*Mytilus*) and 66% initial length (*Limulus*) were fully reversible and took place within the physiological force range. When stretch exceeded two to three times initial length (*Mytilus*) or five to six times initial length (*Limulus*), at forces ~18 nN and ~7 nN, respectively, the filaments broke. Appreciable and reversible strain within the physiological force range implies that thick-filament length changes could play a significant physiological role, at least in invertebrate muscles.

INTRODUCTION

Elastic properties of muscle filaments play a critical role in mechanics. Interpretation of length transients (Ford et al., 1981; Huxley and Tideswell, 1996) for example, has been seriously impacted by recent x-ray diffraction measurements of the extensibility of thin and thick filaments even on the order of less than 0.5% (Huxley et al., 1994; Wakabayashi et al., 1994). These results indicate that a large part (~70%) of the sarcomere's compliance arises from the extensibility of the thin and thick filaments and does not lie in the crossbridges as supposed earlier (Huxley, 1974).

Some attempts have recently been made to approach the issue of filament elasticity by direct measurement. These approaches have employed flexible tapered glass needles (Kishino and Yanagida, 1988; Ishijima et al., 1991), atomic force microscope tips (Rief et al., 1997), and optical traps (Saito et al., 1994; Finer et al., 1995, Depuis et al., 1997; Kellermayer et al., 1997; Tskhovrebova et al., 1997), and have focused either on titin, on actin, or on actin-myosin dynamics. To our knowledge no mechanical studies have been carried out on isolated thick filaments.

We used the new nanofabricated lever force transducers to study thick filaments of two invertebrates, *Mytilus edulis* and *Limulus polyphemus*. When subjected to forces within the ordinary physiological range, filaments of both species could undergo reversible length changes of unexpectedly large magnitude.

Received for publication 6 October 1997 and in final form 4 May 1998.

Address reprint requests to Dr.Thomas Neumann, Department of Bioengineering, University of Washington, Box 357962, Seattle, WA 98195-7962. Tel.: 206-685-2744; Fax: 206-685-300; E-mail: neumann@bioeng.washington.edu.

0006-3495/98/08/938/10 $2.00

MATERIALS AND METHODS

Protein preparation

Mytilus thick filaments were isolated from the anterior byssus retractor (ABRM) of living specimens of the Puget Sound area following the procedure of Sellers et al. (1993). The ABRMs of five precooled mussels were excised and rinsed in buffer D (10 mM ATP, 10 mM $MgCl_2$, 1 mM EGTA, 20 mM MOPS, 3 mM NaN_3, 1 mM dithiothreitol (DTT), and 0.1 mM phenylmethylsulfonyl fluoride (PMSF)) and then homogenized in 5 ml of the same buffer by an Omnimixer. The homogenate was diluted with the same volume of buffer plus 0.1% Triton X-100 (Sigma Chemical Co., St. Louis, MO) for 5 min on ice. Thick filaments could be isolated after three centrifugation cycles alternating between 500 and 5000 × *g*. All steps were carried out by keeping the sample at 4°C. Thick filaments were stored at −20°C in buffer D mixed with glycerol in a ratio of 1:1.

Living horseshoe crabs were purchased from the Marine Biological Laboratory, Woods Hole, MA. Thick filaments were isolated from the telson levator muscles as described by Kensler and Levine (1982) and kept in the freezer in a mixture of relaxing solution (0.1 M KCl, 5 mM $MgCl_2$, 1 mM EGTA, 1 mM DTT, 2.5 mM ATP in 7 mM phosphate buffer, (pH 7.0) mixed with glycerol in a ratio of 1:1.

All thick filament experiments were carried out in Sellers' buffer M (20 mM KCl, 10 mM MOPS, 5 mM $MgCl_2$, 0.1 mM EGTA, 10 mM DTT, 1 mM ATP). The temperature during the experiments was 20–22°C.

Electron microscopy

Isolated *Mytilus* thick filaments were negatively stained with 1% uranyl acetate solution on a copper grid covered by carbon film.

Transducer fabrication and calibration

Force transducers were manufactured using a multi-stage lithographic and etching process at the Cornell Nanofabrication Facility, Ithaca, NY. The process starts with the deposition of a thin silicon nitride film (850 nm) onto a pure silicon wafer. The wafer is coated with photoresist and exposed to light projected through a mask to create an array of small windows. After photoresist development, the areas exposed to light were washed away, effectively transferring the mask pattern into a physical pattern on the wafer. Areas not protected by photoresist were removed, the silicon-nitride layer by a reactive-ion etching (RIE) with CF_4 and the silicon by a wet-etch with KOH.

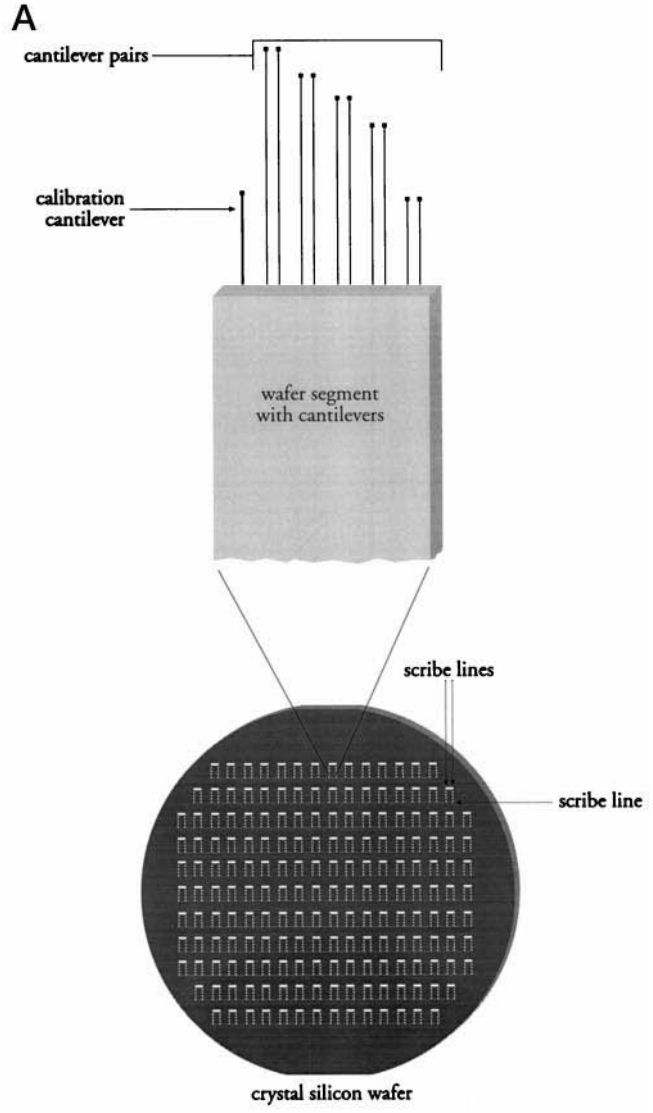

FIGURE 1 (*a*) Drawing of a silicon wafer with multiple windows that contain the cantilevers. The base of each window carries one calibration cantilever and five cantilever pairs of different length. (*b*) Window-base segment containing two cantilever pairs of different length (center, 400 μm; right, 380 μm). The left lever is used only for calibration and is therefore designed stiffer to exclude damping effects. Image obtained using an environmental scanning electron microscope.

After these steps, the wafer was left with a large array of windows, each now containing a free-standing silicon nitride membrane. From these membranes the cantilevers were etched in the following steps. Another mask was created to expose the cantilever pattern in each window. A separate mask was also created so that gold (100-nm thickness) could be deposited (via electron beam evaporation) on the tips of each cantilever to improve optical contrast for imaging. The opposite side of the silicon wafer was coated with photoresist, and this mask pattern was transferred via optical lithography. After final development and RIE, each window was etched, leaving a pattern of cantilevers of different lengths (Fig. 1). Cantilevers were created in pairs so that one member of the pair could be used as a reference for the other. Cantilevers of different stiffness could be used depending on the particular biological sample.

The calibration procedure followed the work of Petersen (1979) and Kiesewetter et al. (1992). Calibration strategy is based on measurement of cantilever dimensions and elastic modulus of the silicon nitride film from which the cantilevers are made. Cantilever length and width were determined using electron microscopy. Thickness was measured using a Leitz film thickness measurement system (MV-SP spectrophotometer). Elastic modulus was determined from resonance-frequency measurements made on a calibration cantilever (Fig. 1 *b*, left) designed to minimize the influence of air damping. The modulus was found to be 204 GPa. This value is presumed the same as the value in nearby regions, from which the longer, more flexible cantilevers are made. From this elastic modulus value and cantilever dimensions, stiffness could be calculated. For the cantilevers used here, stiffness was 0.220 pN/nm. A more detailed description of fabrication and calibration procedures can be found in Fauver et al. (1998).

Transducer implementation

To use the cantilevers in an experiment, a small segment of the wafer was broken along the scribe lines (see Fig. 1 *a*). After cleaning with acetone and alcohol, this small segment was dipped in a solution of 0.2% nitrocellulose (Ernest F. Fullham Inc., Latham, NY) in alcohol, leaving a thin film of nitrocellulose on the cantilevers, which makes their surface more adsorbent to the filaments.

The wafer segment was then glued to the tip of a rod, and the rod was mounted on a hydraulic micromanipulator (Fig. 2). For the reference beam, we applied the same procedure. By micromanipulation, both the rod with the cantilever pair and the rod with the reference beam could then be moved so that their tips were immersed into a drop of thick filament solution that was placed into a small chamber made of Parafilm M (American National Can, Neenah, WI) on a microscope stage coverglass (see Fig. 2).

With the aid of the microscope optics, single thick filaments were caught between a flexible cantilever and a reference beam (cf. Fig. 4, below). For *Mytilus*, we took care that the ends of the filament did not extend over the outer edge of the cantilever tip (width, 3 μm), but we could not determine where exactly on the cantilever tip the filament actually ended. At the opposite end of the filament the overlap could be easily adjusted because reference beam attachment was the final step in the procedure; typically, overlap was ~2 μm. For *Limulus* filaments, the overlap at each end was generally 0.5–1 μm. Because the end regions of the filament overlaid the lever tip, they were not included in the mechanical measurements.

Instrumentation

An inverted microscope (Axiovert 35, Carl Zeiss, Oberkochen, Germany) with a 100× objective (plan-neofluor) was used for differential interfer-

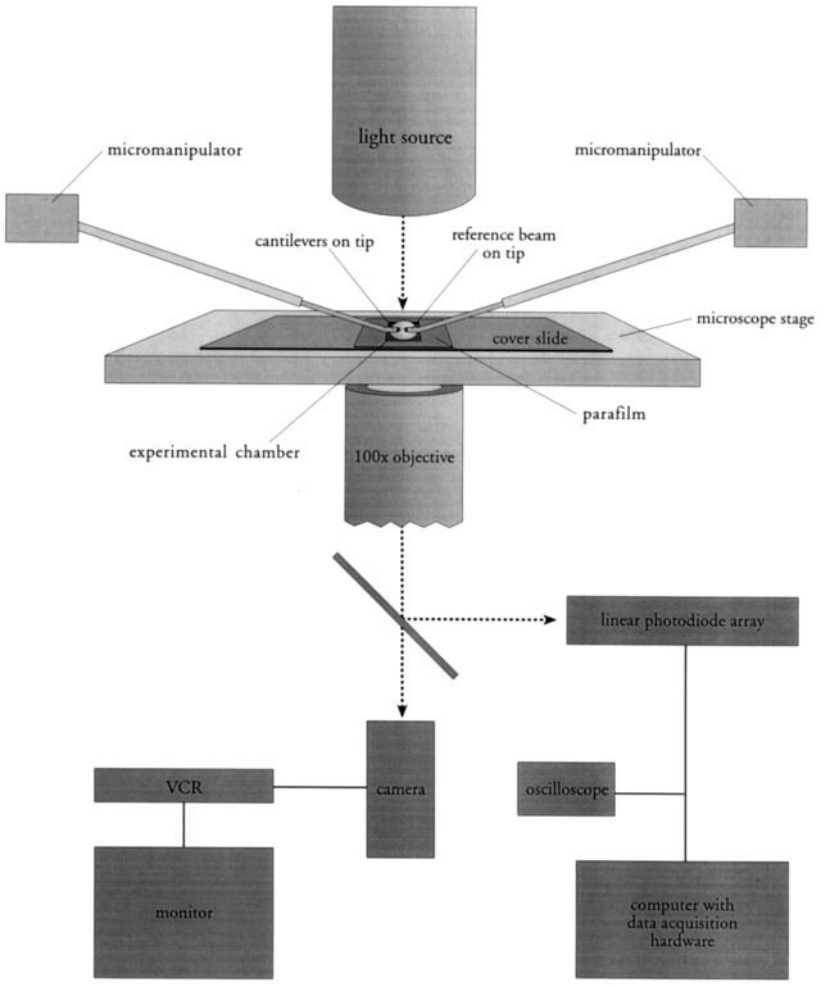

FIGURE 2 Schematic drawing of the experimental setup.

ence contrast imaging. The microscope was placed on a vibration isolation table (Newport Corporation, Irvine, CA). The image was projected onto a CCD camera (Electro-Optical Services, Charlottesville, VA), which was used for visual monitoring. Images were recorded with a SVHS recorder (Mitsubishi BV-1000). Two hydraulic micro-manipulators (Narishige MMW-23) were used to move the cantilevers during the experiment. The positions of the cantilever tips were imaged using a linear photodiode array (Reticon K series 1024 element array, mounted on a Reticon RC0100 motherboard). Data from the photodiode array were acquired using a data acquisition card (National Instruments PC-12000) in a PowerComputing Power Center Pro 180 computer and analyzed using LabVIEW software.

RESULTS

An electron micrograph of *Mytilus* thick filaments similar to those used in the experiments is shown in Fig. 3. The natural variation of filament length and thickness is evident. No actin filaments are visible, implying a fairly pure preparation. In the inset, it is possible to visualize the characteristic molecular surface pattern along the thick filament that is typical of such filaments (Cohen et al., 1971; Szent-Györgyi et al., 1971; Nonomura, 1974; Panté, 1994; Matsuno et al., 1996).

Following the method of Sellers et al. (1993), we checked specimen quality in the in vitro motility assay. Fluorescently labeled actin filaments were added to a solution of *Mytilus* thick filaments. We confirmed that the actin filaments could translate along the thick filaments in an [ATP]-dependent fashion, although no attempt was made to quantitate the measurements. The experiment was performed on *Mytilus* only, as previous attempts to carry out such measurements on *Limulus* had proved unsuccessful (Sellers et al., 1993).

The experimental situation is illustrated in Fig. 4, the left panels showing the actual filament and the right panels schematizing the corresponding experimental maneuvers. In Fig. 4 *a*, the filament is buckled as a result of negative (compressive) force. In Fig. 4 *b*, the cantilever pair has been moved rightward such that the filament is just taut. And in Fig. 4 *c*, the rightward movement is increased such that the filament is stretched. At this stage, the cantilever tips have separated sufficiently that the free cantilever is off the field of view.

Although such video images were used for qualitative and semiquantitative measurements, the ultimate data set was obtained from photodiode array scans, which were also used also to demonstrate the lever system's performance (Fig. 5). Fig. 5 *a* shows a single scan along the photodiode

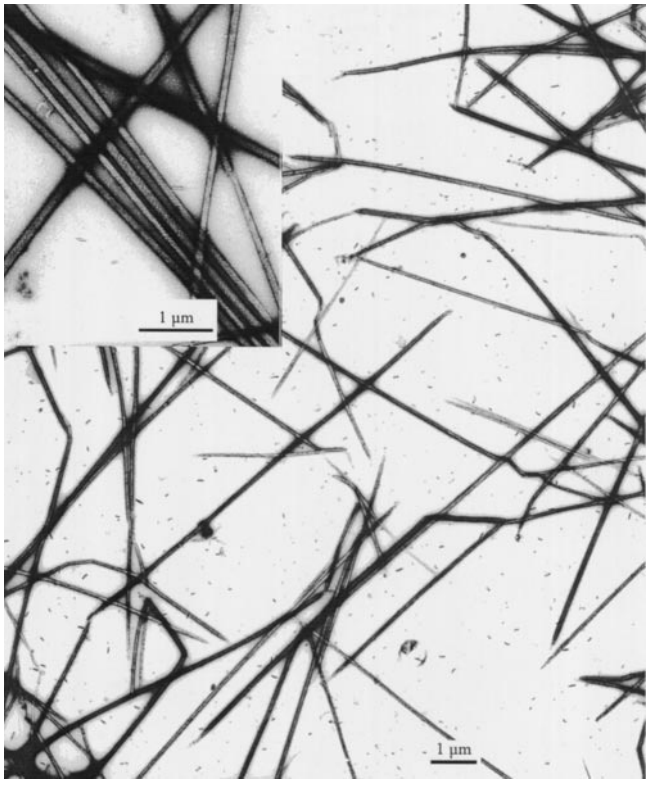

FIGURE 3 Electron micrographs (courtesy of Dr. Károly Trombitás) taken from isolated thick filaments of *Mytilus* after negative staining using 1% uranyl acetate.

array. The scan imaged the two lever tips, marked 1 and 2. Levers were unloaded and immersed in the bathing solution. The centroid position of each tip was computed, and the results are shown as traces 1 and 2 of Fig. 5 *b*. Some drift is apparent, as is noise on the order of 10 nm peak to peak. In the differential signal (2 minus 1), which is used to obtain force, both the noise and the drift are reduced to several nanometers. This performance is several orders of magnitude better than the experiments require.

The time course of filament length change is shown in Fig. 6. The hydraulic manipulator was used to stretch the filament. The top trace shows the position of the free cantilever (x_0), which signals the deflection magnitude. The middle trace shows the position of the cantilever to which the filament is bonded (x_1). The difference in position between top and middle traces gives filament force following the equation: $F = k(|x_1\text{-}x_0| - \text{zero-tension separation of the levers})$. Cantilever stiffness k is given by the dimensions of the rectangular cross section beam and the modulus of elasticity (see Materials and Methods). The bottom trace shows the position of the reference beam. Note that length increases are complete in less than 1 s. After a brief transient, filament force and length show no obvious change.

In a typical experiment, the suspended filament was subjected to several stretch-release cycles of progressively increasing magnitude. This procedure was used to establish the maximal repeatable length change. Data points within each cycle were obtained so as to produce filament length changes on the order of several hundred nanometers between successive points. The time interval between imposed length changes was 30–60 s. Tip separation was also measured before the filament was attached to determine the zero-load span between lever tips.

To obtain a stretch-release cycle, the cantilever pair containing the specimen was first moved toward the reference beam so as to buckle the filament (cf. Fig. 4 *a*). This produced a slightly negative tension. We then began to move the cantilever pair away from the reference beam in increments. The stage of zero tension (levers parallel) was a convenient point to define the filament's initial length. It is important to emphasize that the initial length is smaller than the actual filament length because the end zones of the filament overlaid the levers. Thus, the measurements include nominally the central 50–80% of the filament in *Mytilus* and 25–50% in *Limulus*.

Results obtained from representative *Mytilus* filaments are shown in Fig. 7. Fig. 7 *a* shows three stretch-release cycles, the maximal extent of stretch increasing from cycle to cycle. Note that the return path differs from the extension path, so each force-length loop shows hysteresis. In this particular experiment, the maximal force for the largest loop is 14 nN, which lies within the physiological range (see Discussion).

The repeatability of the length change is better illustrated in Fig. 7 *b*, which shows six stretch-release cycles. After each stretch, the filament recovered within experimental error to its initial length.

In all, 37 experiments were carried out on *Mytilus* thick filaments. Quantitative measurements were based on systematic protocols carried out on the last five. The results were essentially the same in the earlier experiments, although the protocols varied somewhat. For the loops in which stretching was clearly reversible, the average maximal strain was found to be 0.23 (range, 0.13–0.35; $n = 5$ filaments) at a mean tension of 4.8 nN (range, 2.8–6.7 nN). Beyond that, stretch was irreversible and the filament no longer returned to its initial length. Because the gaps between loop size were substantial, the figure for maximal reversible strain is a conservative estimate.

We also measured the yield strength of the single thick filament by stretching until breakage. The filament could be extended by two to three times its initial length before it tore apart. Frequently, just before fracture we could detect a local necking and on occasion a fraying. The maximal force for breakage was typically greater than 18 nN ($n = 4$).

Results obtained on *Limulus* filaments are shown in Fig. 8. The results were essentially similar to those obtained with *Mytilus* (compare Figs. 7 and 8) except that these filaments could be strained considerably more without loss of reversibility. Maximal reversible length change (again a conservative figure because loop sizes were not finely graded) was found to occur at an average strain of 0.66 (range, 0.50–0.95; $n = 5$ measurements with four filaments). At this strain, the mean filament tension was 1.8 nN (range, 1.2–2.8

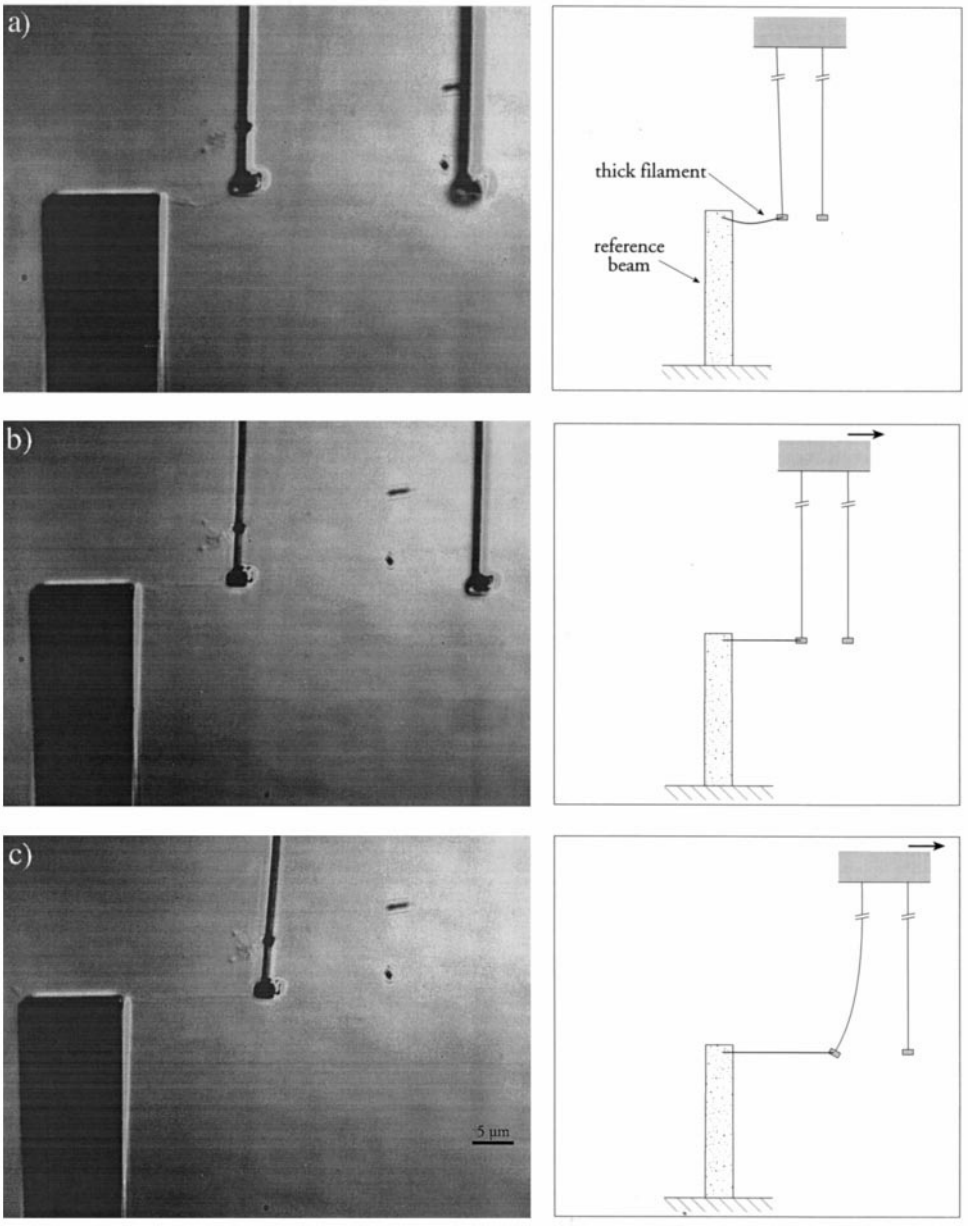

FIGURE 4 Thick filament of *Mytilus* suspended between cantilever and reference beam. In the left column are photographs obtained using differential interference contrast microscopy. In the right column are schematic drawings illustrating corresponding stages of the experiment. Note that levers are considerably longer than shown in the photographs.

nN). *Limulus* filaments could be extended by five to six times their initial length before breaking. Breakage occurred at a tension typically greater than 7 nN.

DISCUSSION

In this study we focused on the elastic properties of single isolated thick filaments. Two types of invertebrate muscle were used, the anterior byssus retractor of the blue mussel *Mytilus edulis* and the telson levator muscle of the horseshoe crab *Limulus polyphemus*. We were curious to determine the extent of strain that might result from stresses comparable to those borne during physiological contraction.

We chose to examine invertebrate thick filaments for two reasons. First, the dimensions are convenient. Thick filaments of *M. edulis* are 10–50 μm long, although because of the limited field of view we used mainly the shorter ones. Thick filaments of *L. polyphemus* are 4–5 μm in length. Thus, optical visibility can be attained without staining or labeling. Second, both of the muscles we selected have been at the center of scientific interest for years, yet many questions about their ultrastructure and working mechanisms remain unanswered, questions about long-term tension maintenance in the catch state (cf. Twarog, 1967; Sobieszek, 1973; Nonomura, 1974; Siegman et al., 1997) and questions about thick filament shortening (de Villafranca and Marschhaus, 1963; Dewey et al., 1977; Levine and Kensler, 1985; Levine et al., 1991).

Although we were quite prepared to look for length changes on the order of 1% or less (Fig. 5), in both types of specimen we found that thick filaments were able to undergo repeatable length changes of substantially larger mag-

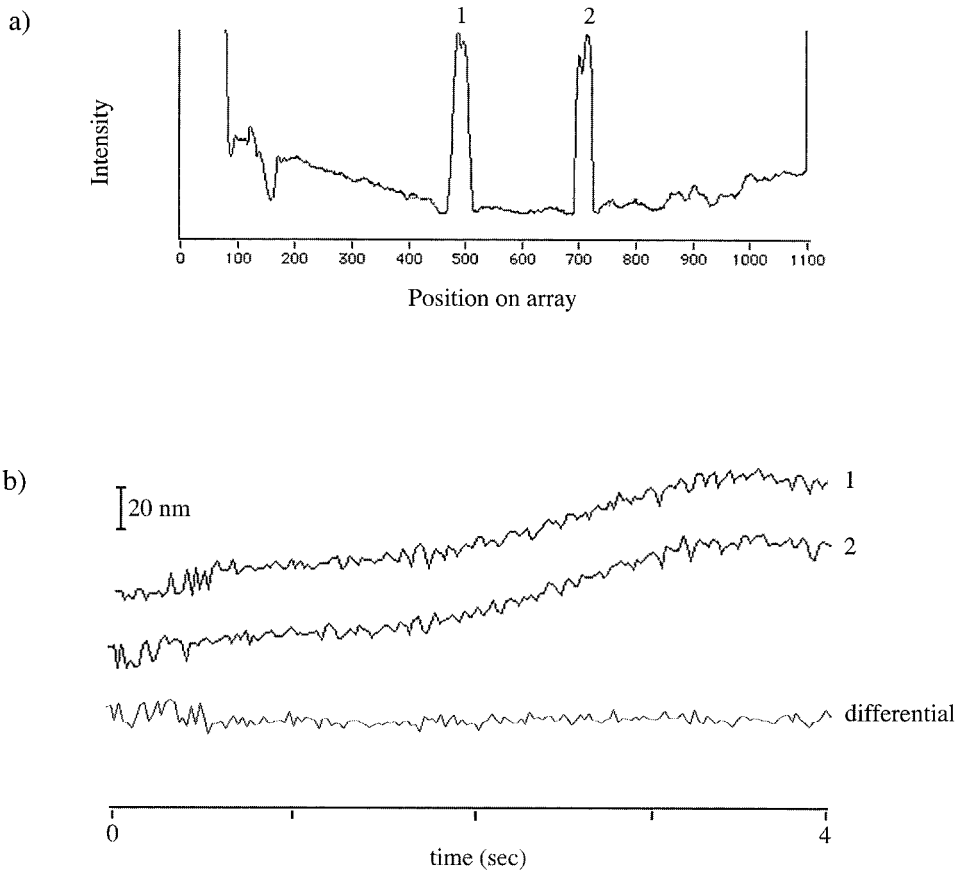

FIGURE 5 Performance of the levers (stiffness, 0.31 pN/nm). (*a*) Image of the two lever tips on the photodiode array. (*b*) Computed centroid position of each tip (traces 1 and 2). The differential signal (trace 2 minus 1) reduces noise and drift.

nitude. In isolated thick filaments of *Mytilus* the repeatable length change was 23% and in *Limulus* the change was 66%.

One issue is whether the filaments under study were physiological. Filaments were prepared by standard methods. Their ultrastructure (Fig. 3) was similar to that commonly reported, and as far as we could tell from the in vitro motility assay the filaments were functional. Thus, we have no reason to suspect damage. Furthermore, the thick filaments' end regions overlapped the cantilever surface in a

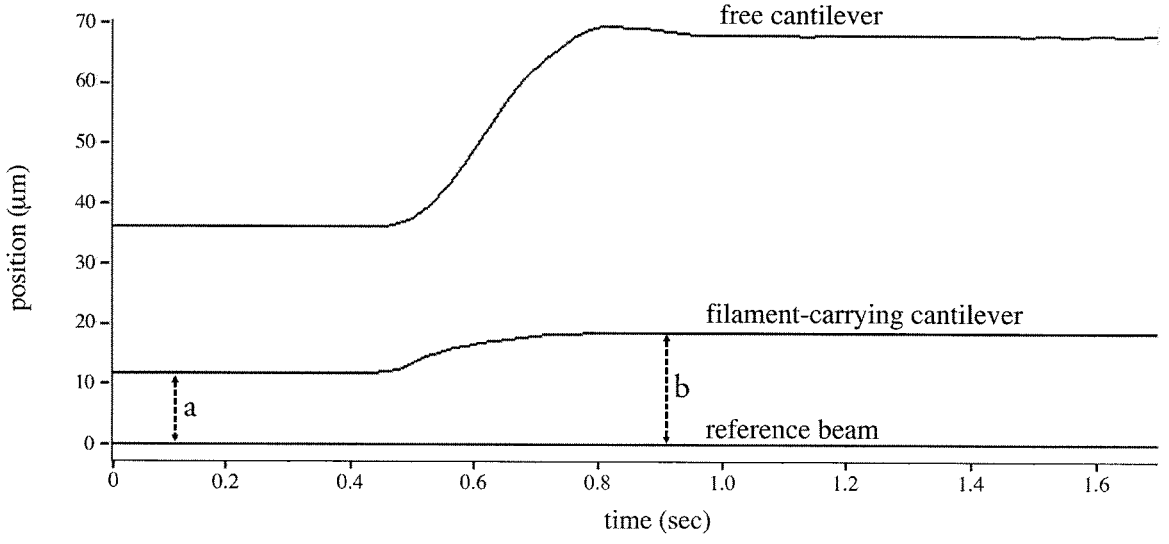

FIGURE 6 Time course of length change imposed on a 15–16-μm-long *Mytilus* thick filament by rapid manual micromanipulator movement. Computed positions of the free cantilever (*top*), the cantilever with the attached filament (*middle*), and the reference beam (*bottom*) are shown. A 12-μm segment of the filament was included in the stretch, as indicated by *a*. This segment was extended by ~58% (*b*). Data were obtained from the photodiode array.

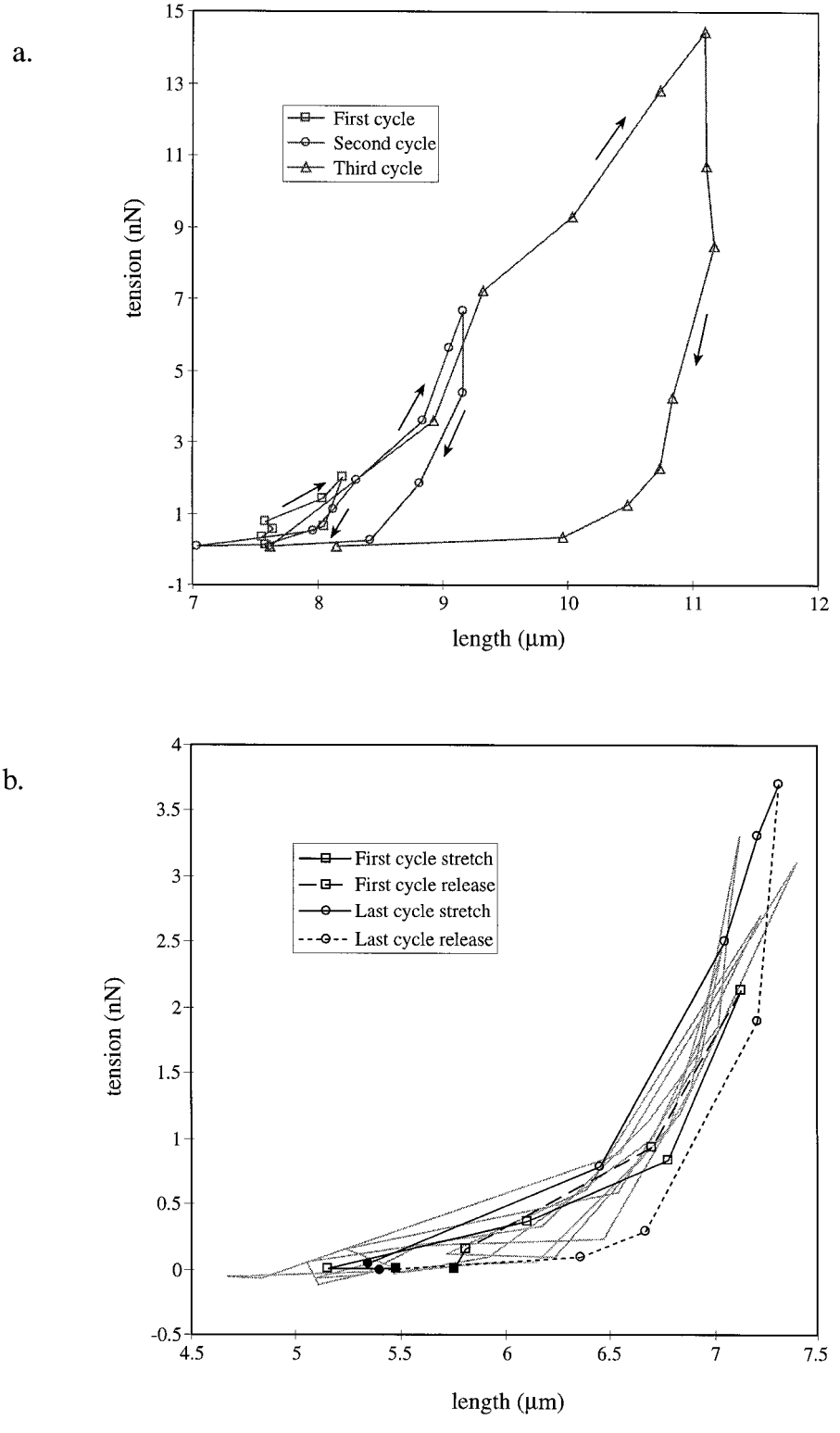

FIGURE 7 Results on single *M. edulis* thick filaments. (*a*) Length-tension diagram showing three successive stretch-release cycles of increasing magnitude. (*b*) Six successive stretch-release cycles of the same magnitude. First and last cycles are highlighted, with beginning and end points indicated by filled symbols.

manner comparable to the way end regions overlap thin filaments in the sarcomere. Transmission of force may therefore be not far from physiological. One uncertainty, particularly with *Limulus*, is that it is possible that two filaments were occasionally suspended instead of one, which would affect tension values but not strain values.

The force required to produce the reversible extension lies within the physiological range. To estimate the physiological tension maximum per thick filament, one can simply take the published value of active tension per cross section and divide by the cross-sectional density of thick filaments. For *Mytilus* ABRM, the physiological tension is

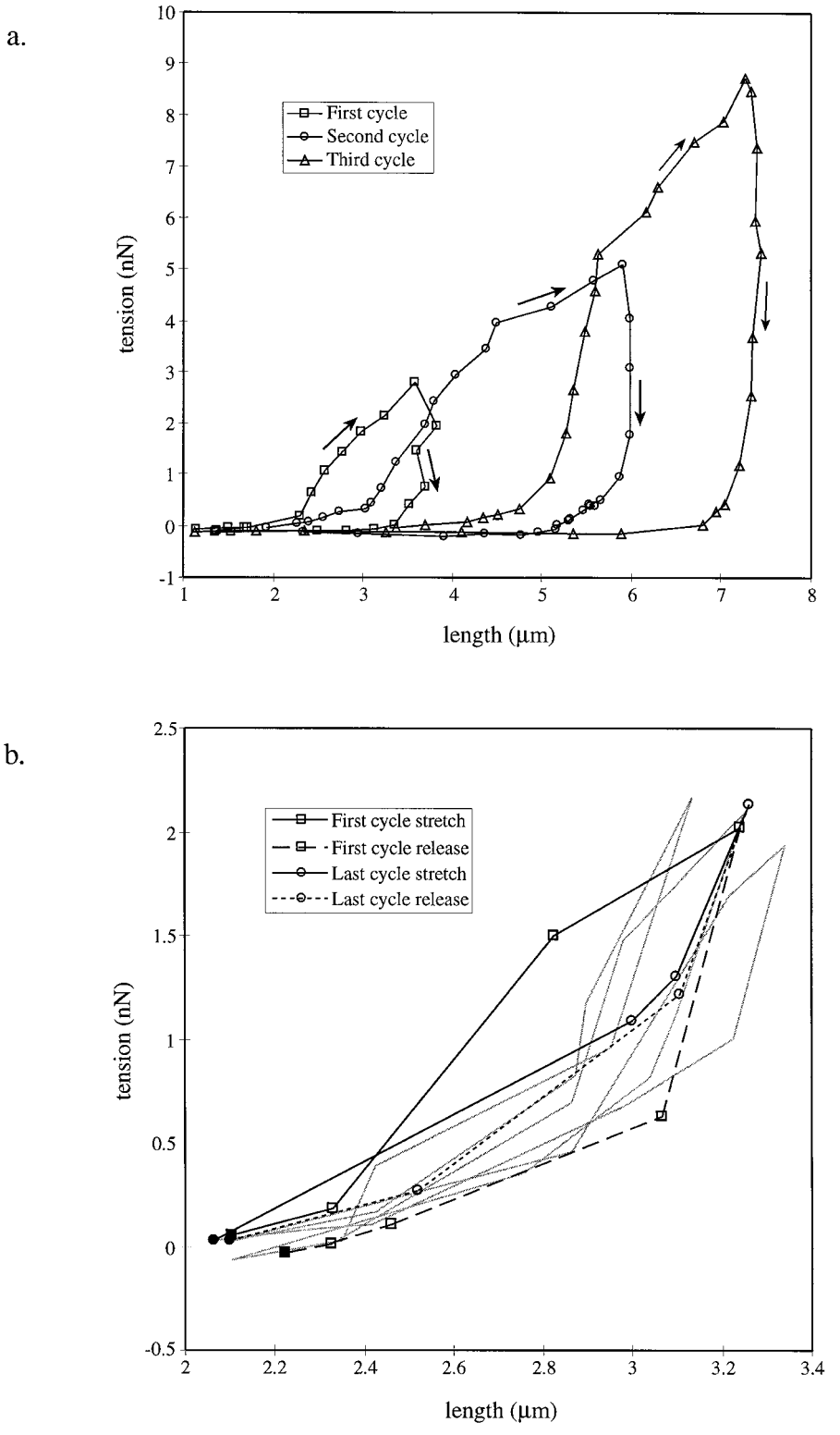

FIGURE 8 Results on single *L. polyphemus* thick filaments. (*a*) Length-tension diagram showing three successive stretch-release cycles of progressively increasing magnitude. (*b*) Five successive stretch-release cycles of the same magnitude. First and last cycles are highlighted, with beginning and end points indicated by filled symbols.

reported to be in the range of 86 g/mm^2 (Lowy and Millman, 1963), 100–120 g/mm^2 (Twarog, 1967), and 66.7–104.7 g/mm^2 (Chick and Stephenson, 1995). Estimates of the number of thick filaments per unit cross-sectional area were obtained from transmission electron micrographs (courtesy Dr. Károly Trombitás). The thick filament density was counted to be 5.5×10^7 per mm^2. This value is an estimate, for the interfilament spacing will vary somewhat with sarcomere length and preparative procedures. From the values of filament density and tension we calculated the maximal contractile force per thick filament to be 12–21 nN. From measurements on rapidly frozen ABRM samples,

Bennett and Elliott (1989) reported the active force per single thick filament to be ~8 nN. Their value is lower than the 12–21 nN calculated but still exceeds the mean force (4.8 nN) that was required to produce maximal reversible filament strain. Thus, the applied force levels were squarely within the physiological range.

For *Limulus*, the maximal tension during contraction is reported to be 0.34 N/mm^2 (Walcott and Dewey, 1980). Using a published cross-sectional electron micrograph of *Limulus* muscle (Eagles et al., 1982) we counted the thick filaments in the same way as described for *Mytilus*. This gave a value of 1.23×10^8 thick filaments/mm^2, which corresponds to 2.8 nN/thick filament. A second count in a different region of the micrograph gave a value of 6.98×10^7 thick filaments/mm^2, which corresponds to 4.9 nN/thick filament. Thus, there is considerable variation. Notwithstanding this uncertainty, the maximal tension (1.8 nN) for reversible length change nevertheless appears to lie well within the physiological range.

The results raise the question of how in situ filaments could sustain a constant length physiologically while subject to forces similar to those imposed here. There is evidence for filament length constancy in situ. In ABRM, Millman and Elliott (1972) found that the spacing of the meridional x-ray reflections remained constant as the specimen passed from relaxation to contraction. In *Limulus*, Levine and Kensler (1985) and Levine et al. (1991) investigated optical transforms of isolated thick filaments, and although the contracted filaments were ~25% shorter than relaxed ones, molecular arrangements appeared no different. Thus, published evidence implies no contraction-dependent molecular rearrangements in situ, whereas the present results imply that some molecular arrangement could in fact be taking place.

There seem to be several possibilities to explain this discrepancy. One possibility is that thick filaments do actually lengthen during in situ contraction, the above results notwithstanding. We are not referring to the 0.3% length change reported in ABRM (Tajima et al., 1994) and other species, but to changes of the same large magnitude as found here. This possibility is not necessarily out of accord with the results cited above as the diffraction patterns come mainly from ordered regions of the filaments. If thick filaments lengthened by molecular transformations in specific zones along the filament (Pollack, 1990), which then became disordered, these zones would no longer contribute. The patterns would derive only from the zones that did not change length and remained ordered. The pattern would weaken (as observed) because of a diminished number of contributing elements. Such a result might be interpreted as filament length constancy, whereas in fact the filament could have lengthened. Thus, the possibility of filament lengthening in situ is not easy to rule out. Indeed, experiments of Sugi and Gomi (1981) carried out on the horseshoe crab revealed that during isometric contraction the A-band width increased by 10%.

Another possibility is that thick filaments do not lengthen during contraction in situ, but may actually shorten and generate active tension. Although the prevailing view is that filaments do not shorten, there is evidence to the contrary (Pollack, 1983). In one model (Pollack, 1990), relaxed filaments are relatively rigid, sustaining physiological forces with strain of $<1\%$, whereas shortened filaments are highly compliant because the α-helical rods comprising the filament backbone have undergone helix-coil transition (Harrington, 1971). Thus, compliance of the shortened filament is qualitatively different from compliance of the relaxed filament. If filament shortening were triggered either by the procedure of isolating the filaments or by the procedure of mounting the filaments on the nanolevers, it may be that the filaments under investigation were in the pre-shortened state; thus, the applied stress would have relengthened the filaments toward their initial length. Whether this is the correct explanation or the one in the previous paragraph is correct, or indeed whether yet another explanation is correct, awaits the results of further experimentation. The only conclusion of some certainty is that single filaments in vitro are capable of considerable reversible elastic extension under physiological load.

In addition to examining filament compliance, we also studied the filaments' yield strength, i.e., the force required to break the filament. For *Mytilus* filaments, the yield strength was >18 nN, and for *Limulus* it was >7 nN. Although the accuracy of these measurements was limited, it seemed clear that the breaking strength is only modestly higher than physiological forces, and not orders of magnitude higher.

Beyond the specific physiological implications, the results demonstrate the first systematic application of nanofabricated force transducers for biological measurement. These transducers are relatively simple to use and their calibration is easy and precise (Fauver et al., 1998). They can be fabricated in various shapes and sizes dictated by the requirements of the particular experiment. It is clear from Fig. 5 that resolution is excellent. For these reasons, nanofabricated cantilevers may prove to be a good alternative to other methods such as ultrathin glass needles, atomic force microscopes, and optical tweezers to measure forces at the near-molecular level.

We thank Sarah Richards for creating the graphics, Kyung Hee Lee and Martin Aichele for assistance with transducer implementation and protein preparation, John Myers and Jeff Magula for technical help, and Dr. Károly Trombitás for preparing the electron micrographs.

REFERENCES

Bennett, P. M., and A. Elliot. 1989. The 'catch' mechanism in molluscan muscle: an electron microscopy study of freeze substituted anterior byssus retractor muscle of *Mytilus edulis*. *J. Muscle Res. Cell Motil.* 10:297–311.

Chick, J. J., and D. G. Stephenson. 1995. The effect of temperature on contractile activation of intact and chemically skinned 'catch' muscle fiber bundles of *Mytulis edulis*. *J. Muscle Res. Cell Motil.* 16:285–294.

Cohen, C., A. G. Szent-Gyorgyi, and J. Kendrick-Jones. 1971. Paramyosin and the filaments of molluscan 'catch' muscles. I. Paramyosin: structure and assembly. *J. Mol. Biol.* 56:223–237.

Depuis, D. E., W. H. Guilford, J. Wu, and D. M. Warshaw. 1997. Actin filament mechanics in the laser trap. *J. Muscle Res. Cell Motil.* 18: 17–30.

de Villafranca, G. W., and C. E. Marschhaus. 1963. Contraction of the A band. *J. Ultrastruct. Res.* 9:156–165.

Dewey, M. M., D. E. Walcott, D. E. Colflesh, H. Terry, and R. J. C. Levine. 1977. Changes in thick filament length in *Limulus* striated muscle. *J. Cell Biol.* 75:366–380.

Eagles, D. A., G. A. De Andrea, and G. P. Riordan. 1982. The T-axial membrane system in striated muscles of the horseshoe crab. *Tissue Cell* 14:531–540.

Fauver, M., D. Dunaway, D. Lilienfeld, H. Craighead, and G. Pollack. 1998. Microfabricated cantilevers for measurement of subcellular and molecular forces. *IEEE Trans. Biomed. Eng.* 45:891–898.

Finer, J. T., A. D. Mehta, and J. A. Spudich. 1995. Characterization of single actin-myosin interactions. *Biophys. J.* 68:291s–297s.

Ford, L. E., A. F. Huxley, and R. M. Simmons. 1981. The relation between stiffness and filament overlap in stimulated frog muscle fibres. *J. Physiol.* 311:219–249.

Harrington, W. F. 1971. A mechanochemical mechanism for muscle contraction. *Proc. Natl. Acad. Sci. U.S.A.* 6:685–689.

Huxley, A. F. 1974. Muscular contraction. *J. Physiol.* 243:1–43.

Huxley, H. E., A. Stewart, H. Sosa, and T. Irving. 1994. X-ray diffraction measurements of the extensibility of actin and myosin filaments in contracting muscle. *Biophys. J.* 67:2411–2421.

Huxley, A. F., and S. Tideswell. 1996. Filament compliance and tension transients in muscle. *J. Muscle Res. Cell Motil.* 17:507–511.

Ishijima, A., T. Doi, K. Sakurada, and T. Yanagida. 1991. Sub-piconewton force fluctuations of actomyosin *in vitro*. *Nature.* 352:301–306.

Kellermayer, M. S., S. B. Smith, H. L. Granzier, and C. Bustamante. 1997. Folding-unfolding transitions in single titin molecules characterized with laser tweezers. *Science.* 276:1112–1116.

Kensler, R. W., and R. J. C. Levine. 1982. An electron microscopic and optical diffraction analysis of the structure of *Limulus* telson muscle thick filaments. *J. Cell Biol.* 92:443–451.

Kiesewetter, L., J. M. Zang, D. Houdeau, and A. Steckenboom. 1992. Determination of Young's moduli of micromechanical thin films using the resonance method. *Sensors Actuators A.* 35:153–159.

Kishino, A., and T. Yanagida. 1988. Force measurements by micromanipulation of a single actin filament by glass needles. *Nature.* 334:74–76.

Levine, R. J. C., and R. W. Kensler. 1985. Structure of short thick filaments from *Limulus* muscle. *J. Mol. Biol.* 182:347–352.

Levine, R. J. C., J. L. Woodhead, and H. A. King. 1991. The effect of calcium activation of skinned fiber bundles on the structure of Limulus thick filaments. *J. Cell. Biol.* 113:573–583.

Lowy, J., and B. M. Millman. 1963. The contractile mechanism of the anterior byssus retractor muscle of *Mytilus edulis*. *Philos. Trans. R. Soc. Lond. B.* 246:105–148.

Matsuno, A., M. Kannda, and M. Okuda. 1996. Ultrastructural studies on paramyosin core filaments from native thick filaments in catch muscles. *Tissue Cell*. 28:501–505.

Millman, B. M., and G. F. Elliott. 1972. An x-ray diffraction study of contracting molluscan smooth muscle. *Biophys. J.* 12:1405–1413.

Nonomura, Y. 1974. Fine structure of the thick filament in molluscan catch muscle. *J. Mol. Biol.* 88:445–455.

Panté, N. 1994. Paramyosin polarity in the thick filament of molluscan smooth muscles. *J. Struct. Biol.* 113:148–163.

Petersen, K. E. 1979. Young's modulus measurements of thin films using micromechanics. *J. Appl. Phys.* 50:6761–6766.

Pollack, G. H. 1983. The cross-bridge theory. *Phys. Rev.* 63:1049–1113.

Pollack, G. H. 1990. Muscles and Molecules: Uncovering the Principles of Biological Motion. Ebner and Sons, Seattle, WA.

Rief, M., M. Gautel, F. Oesterheld, J. M. Fernandez, and H. E. Gaub. 1997. Reversible unfolding of individual titin immunoglobulin domains by AFM. *Science.* 276:1090–1092.

Saito, K., A. Takaaki, T. Aoki, and T. Yanagida. 1994. Movement of single myosin filaments and myosin step size on an actin filament suspended in solution by a laser trap. *Biophys. J.* 66:769–777.

Sellers, J. R., G. Cuda, F. Wang, and E. Homsher. 1993. Myosin-specific adaptations of the motility assay. *Methods Cell Biol.* 39:23–49.

Siegman, M. J., S. U. Mooers, C. Li, S. Narayan, L. Trincle-Mulcahy, S. Wataba, D. J. Hartshorne, and T. Butler. 1997. Phosphorylation of a high molecular weight (~600 kDa) protein regulates catch in invertebrate smooth muscle. 1997. *J. Muscle Res. Cell Motil.* 18:655–670.

Sobieszek, A. 1973. The fine structure of the contractile apparatus of the anterior byssus retractor muscle of *Mytilus edulis*. *J. Ultrastruct. Res.* 43:313–343.

Sugi, H., and G. Gomi. 1981. Changes in the A-band width during contraction in horseshoe crab striated muscle. *Experimentia.* 37:65–67.

Szent-Györgyi, A. G., C. Cohen, and J. Kendrick-Jones. 1971. Paramyosin and the filaments of molluscan 'catch' muscles. II. Native filaments: isolation and characterization. *J. Mol. Biol.* 56:239–258.

Tajima, Y., K. Makino, T. Hanyuu, K. Wakabayashi, and Y. Amemiya. 1994. X-ray evidence for the elongation of thick and thin filaments during isometric contraction of a molluscan smooth muscle. *J. Muscle Res. Cell Motil.* 15:659–671.

Tskhovrebova, L., J. Trinick, J. A. Sleep, and R. M. Simmons. 1997. Elasticity and unfolding of the single molecules of the giant muscle protein titin. *Nature.* 387:308–312.

Twarog, B. M. 1967. The regulation of catch in molluscan muscle. *J. Gen. Physiol.* 50:157–167.

Wakabayashi, K., Y. Sugimoto, H. Tanaka, Y. Ueno, Y. Takezawa, and Y. Amemiya. 1994. X-ray diffraction evidence for the extensibility of actin and myosin filaments during muscle contraction. *Biophys. J.* 67: 2422–2435.

Walcott, B., and M. M. Dewey. 1980. Length-tension relation in *Limulus* striated muscle. *J. Cell Biol.* 87:204–208.